

## Characterization of Singly Reduced Iron(II) Porphyrins

Robert J. Donohoe, Michael Atamian, and David F. Bocian\*

Contribution from the Department of Chemistry, Carnegie Mellon University, Pittsburgh, Pennsylvania 15213. Received February 17, 1987

**Abstract:** Optical absorption, electron paramagnetic resonance (EPR), and resonance Raman (RR) spectra are reported for the one-electron reduction products of a series of Fe<sup>II</sup> porphyrins. The porphyrins include 5,10,15,20-tetraphenylporphyrin (TPP), 2,7,12,17-tetrabromo-5,10,15,20-tetraphenylporphyrin (TPPBr<sub>4</sub>), 2,7,12-tricyano-5,10,15,20-tetraphenylporphyrin (TPP(CN)<sub>3</sub>), and 2,7,12,17-tetracyano-5,10,15,20-tetraphenylporphyrin (TPP(CN)<sub>4</sub>). The iron complexes of these porphyrins represent a series in which the reduction potential is successively shifted to more positive values. The RR and EPR data demonstrate that for all of the complexes reduction results in a low-spin configuration for the metal ion. For [FeTPP]<sup>-</sup> and [FeTPPBr<sub>4</sub>]<sup>-</sup>, the unpaired electron resides in the metal d<sub>z<sup>2</sup></sub> orbital; however, reduction results in the transfer of a significant amount of paired electron density to the macrocycle through π back-bonding. Destabilization of the metal d<sub>z<sup>2</sup></sub> orbital via ligation of a single pyridine or CO molecule is insufficient to "push" the unpaired electron from the metal ion to the macrocycle. For [FeTPP(CN)<sub>3</sub>]<sup>-</sup> and [FeTPP(CN)<sub>4</sub>]<sup>-</sup>, the unpaired electron resides primarily on the porphyrin ring although a small amount of unpaired density is shared with the metal ion through π-orbital interactions. The extensive interaction between the metal and porphyrin π orbitals which is present in all of the complexes provides a mechanism for enhancing the oscillator strength of formally forbidden charge-transfer transitions. It is suggested that these charge-transfer absorptions are primarily responsible for the complicated optical spectra of the reduced complexes.

## I. Introduction

Iron(II) porphyrins (Fe<sup>II</sup>-P) reduced by one electron are of interest due to their possible involvement in the catalytic cycle of redox proteins and their potential utility in synthetic schemes.<sup>1-5</sup> A number of spectroscopic techniques and physical measurements (electron paramagnetic resonance (EPR),<sup>5-8</sup> electronic absorption (UV-vis),<sup>6,9-11</sup> Mössbauer,<sup>9</sup> nuclear magnetic resonance (NMR),<sup>12</sup> and resonance Raman (RR) spectroscopy;<sup>8,13</sup> magnetic susceptibility,<sup>5,9,12</sup> electrochemistry,<sup>6,14,15</sup> and X-ray crystallography<sup>16</sup>) have been used in an effort to characterize these systems. Nevertheless, the question remains as to whether the one-electron reduction products are best described as d<sup>7</sup> iron(I) porphyrins ([Fe<sup>I</sup>-P]<sup>-</sup>), porphyrin π-anion radicals ([Fe<sup>II</sup>-P\*]<sup>-</sup>) or a form intermediate between these two limiting cases.<sup>9</sup> Some of the difficulty in adequately describing the [Fe-P]<sup>-</sup> complexes may be due to the fact that, to date, only two complexes, [FeTPP]<sup>-</sup> (TPP = tetraphenylporphyrin) and [FeOEP]<sup>-</sup> (OEP = octaethylporphyrin), have been examined in detail. A predominantly [Fe<sup>I</sup>-P]<sup>-</sup> description of these complexes is supported by the EPR, NMR, RR, and Mössbauer data while a predominantly [Fe<sup>II</sup>-P\*]<sup>-</sup>

**Table I.** Half-Wave Potentials ( $E_{1/2}$ )<sup>a</sup> for the Iron Porphyrin (Fe-P) Complexes Examined in This Study

complex	redox couple ( $E_{1/2}$ )		
	[Fe-P] <sup>+</sup> / Fe-P	Fe-P/ [Fe-P] <sup>-</sup>	[Fe-P] <sup>-</sup> / [Fe-P] <sup>2-</sup>
FeTPP	-0.121	-0.986	-1.633
FeTPPBr <sub>4</sub>	0.083	-0.812	-1.260
FeTPP(CN) <sub>3</sub>	0.185	-0.539	-0.974
FeTPP(CN) <sub>4</sub>	0.215	-0.475	-0.865

<sup>a</sup> Potentials listed are V vs. Ag/AgCl.

formulation is suggested by the UV-vis and crystallographic studies.

While [FeTPP]<sup>-</sup> and [FeOEP]<sup>-</sup> are the most-studied [Fe-P]<sup>-</sup> complexes, limited spectral data are available for other reduced systems; of particular note is the β-cyano-substituted TPP complex, [FeTPP(CN)<sub>4</sub>]<sup>-</sup>.<sup>15,17</sup> The EPR spectrum of this complex is characteristic of a porphyrin π-anion radical, unlike the spectra of either [FeTPP]<sup>-</sup> or [FeOEP]<sup>-</sup>. This suggests that substituent groups can dramatically influence the electron distribution in the [Fe-P]<sup>-</sup> complexes. The fact that the [Fe-P]<sup>-</sup>/[Fe-P]<sup>-</sup> redox couple for FeTPP(CN)<sub>4</sub> is substantially shifted toward positive potential relative to either FeTPP or FeOEP further suggests that it may be possible to manipulate the electron distribution in the [Fe-P]<sup>-</sup> complexes by addition of substituent groups which vary this redox couple.

In this paper, we examine the UV-vis, EPR, and RR spectra of the one-electron reduction products of the series of Fe<sup>II</sup>TPP derivatives shown in Figure 1. The redox couples (below 0.3 V) for the molecules shown in the figure are listed in Table I. As can be seen, the [Fe<sup>II</sup>-P]/[Fe-P]<sup>-</sup> couple varies in a stepwise manner from -0.986 to -0.475 V (V vs. Ag/AgCl). The shift of this couple toward positive potential is due to the presence of electron-withdrawing groups on the macrocycle. Electron-withdrawing groups at the β-pyrrole positions primarily stabilize the porphyrin e<sub>g</sub>\* orbitals<sup>18</sup> which would serve as the redox orbitals for macrocycle-centered reductions. In addition, perturbation of the e<sub>g</sub>\* orbitals indirectly influences the metal d<sub>z<sup>2</sup></sub> orbitals due to symmetry equivalence. The metal orbital energies can be directly perturbed by the presence of axial ligands. Such ligands primarily destabilize the metal d<sub>z<sup>2</sup></sub> orbital which could serve as the redox

(1) Collman, J. P.; Sorrell, T. N.; Dawson, J. H.; Trudel, R. J.; Bunnenberg, E.; Djerassi, C. *Proc. Natl. Acad. Sci. U.S.A.* **1976**, *73*, 6-10.

(2) Reed, C. A.; Mashiko, T.; Scheidt, W. R.; Haller, K. *First International Symposium on O<sub>2</sub> Activation and Selective Oxidations Catalyzed by Transition Metals*; Bendor, France, 1979; Poster abstract.

(3) Welborn, C. H.; Dolphin, D.; James, B. R. *J. Am. Chem. Soc.* **1981**, *103*, 2869-2871.

(4) Lexa, D.; Saveant, J.-M. *J. Am. Chem. Soc.* **1982**, *104*, 3503-3504.

(5) Cohen, I. A.; Ostfeld, D.; Lichenstein, B. *J. Am. Chem. Soc.* **1972**, *94*, 4522-4525.

(6) Lexa, D.; Momenteau, M.; Mispelter, J. *Biochim. Biophys. Acta* **1974**, *338*, 151-153.

(7) Kadish, K. M.; Larson, G.; Lexa, D.; Momenteau, M. *J. Am. Chem. Soc.* **1975**, *97*, 282-288.

(8) Srivatsa, G. S.; Sawyer, D. T.; Boldt, N. J.; Bocian, D. F. *Inorg. Chem.* **1985**, *24*, 2123-2125.

(9) Reed, C. A. *Adv. Chem. Ser.* **1982**, 333-356.

(10) Jones, S. E.; Srivatsa, G. S.; Sawyer, D. T.; Traylor, T. G.; Mincey, T. C. *Inorg. Chem.* **1983**, *22*, 3903-3910.

(11) Brault, D.; Santus, R.; Land, E. J.; Swallow, A. J. *J. Phys. Chem.* **1984**, *88*, 5836-5840.

(12) Hickman, D. L.; Shirazi, A.; Goff, H. M. *Inorg. Chem.* **1985**, *24*, 563-566.

(13) Teraoka, J.; Hashimoto, S.; Sugimoto, H.; Mori, M.; Kitagawa, T. *J. Am. Chem. Soc.* **1987**, *109*, 180-184.

(14) Kadish, K. M. In *Iron Porphyrins*; Lever, A. B. P., Gray, H. B., Eds.; Addison-Wesley: Reading, MA, 1983; Vol. II, pp 161-249.

(15) Giraudeau, A.; Callot, H. J.; Jordan, J.; Ezhar, I.; Gross, M. *J. Am. Chem. Soc.* **1979**, *101*, 3857-3862.

(16) Mashiko, T.; Reed, C. A.; Haller, K. J.; Scheidt, W. R. *Inorg. Chem.* **1984**, *23*, 3192-3196.

(17) Kadish, K. M.; Boisselier-Cocolios, B.; Simonet, B.; Chang, D.; Ledon, H.; Cocolios, P. *Inorg. Chem.* **1985**, *24*, 2148-2156.

(18) Giraudeau, A.; Louati, A.; Gross, M.; Callot, H. J.; Hanson, L. K.; Rhodes, R. K.; Kadish, K. M. *Inorg. Chem.* **1982**, *21*, 1581-1586.

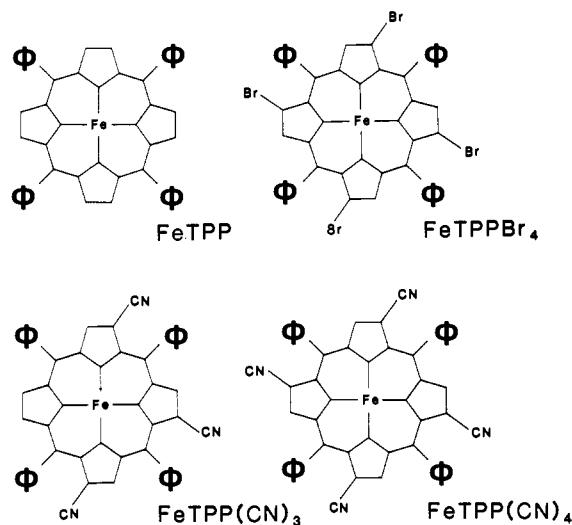


**Figure 1.** Structures of the  $\beta$ -substituted iron porphyrins examined in this study.

orbital for a metal-centered reduction. Accordingly, we also examine the effects of addition of axial ligands on the spectral properties of the  $[\text{Fe-P}]^-$  complexes. In this manner, we probe the electron-density distribution as a function of both the porphyrin and metal orbital energies. The EPR and RR techniques were chosen because they provide complementary information about the electronic distributions in the reduced systems. The EPR spectrum primarily reflects the properties of the metal ion while the RR spectrum primarily measures the properties of the porphyrin macrocycle.<sup>19</sup>

## II. Experimental Section

Tetraphenylporphyrin (chlorin free) was obtained from Mid-century (Posen, IL) and used as received. The  $\beta$ -substituted porphyrins were synthesized according to the procedure given by Callot<sup>20,21</sup> except that the separations were accomplished on a Harrison Research Model 7924T Chromatotron. The brominated porphyrins were eluted with  $\text{CCl}_4/\text{C}_6\text{H}_6$  (3:2) while the cyano-substituted molecules were eluted with  $\text{CH}_2\text{Cl}_2$ . HPLC, TLC, and UV-vis spectroscopy confirmed the presence of a single component. Iron and zinc porphyrins were prepared and purified according to published procedures.<sup>22</sup> The absorption maxima (nm) for the iron porphyrins in  $\text{CH}_2\text{Cl}_2$  are as follows:  $\text{FeTPP-Br}_4\text{Cl}$ , 436, 525, 605;  $\text{FeTPP}(\text{CN})_3\text{Cl}$ , 440, 598, 652;  $\text{FeTPP}(\text{CN})_4\text{Cl}$ , 445, 602, 630. Low-spin  $\text{Fe}^{\text{II}}$  porphyrins were prepared by adding an excess of imidazole, Im (Sigma, recrystallized twice from benzene), to the solutions. All porphyrin reactions and separations were performed under nitrogen or argon in subdued light. All solvents were reagent grade and distilled prior to use.

The reduced complexes were prepared electrochemically in a nitrogen atmosphere glovebox in which extreme care was taken to minimize oxygen levels. Reductions were accomplished in standard three-compartment cells with platinum working and counter electrodes and a  $\text{Ag}/\text{AgCl}$  reference. Cyclic voltammograms and bulk electrolyses were performed by using a Princeton Applied Research (PAR) Model 175 Universal Programmer in conjunction with a PAR Model 173 potentiostat. RR data were obtained in situ by using an airtight electrochemical cell<sup>23</sup> which was prepared in the glovebox. In all cases, *N,N*-dimethylformamide, DMF (Fisher Reagent Grade, stored over

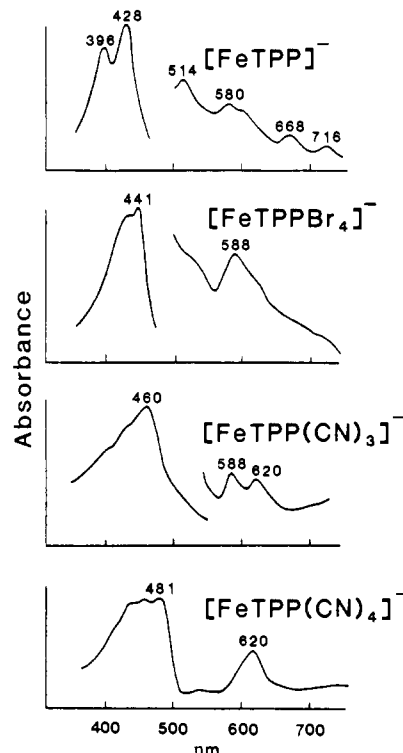


**Figure 2.** Absorption spectra of the  $[\text{Fe-P}]^-$  complexes in DMF, 0.1 M TBAP. Concentrations were approximately  $3 \times 10^{-4}$  M for the Soret region and  $1 \times 10^{-3}$  M for the visible region.

4 Å molecular sieves and distilled in vacuo), was the solvent with tetrabutylammonium perchlorate, TBAP (Kodak, recrystallized twice from absolute ethanol and dried at 111 °C in vacuo), used as supporting electrolyte ( $\sim 0.1$  M). The integrity of the reduced complexes was monitored by cyclic voltammetry, coulometry, and UV-vis spectroscopy.

The axial ligation of the reduced porphyrins by carbon monoxide (Matheson Research Grade 99.99%) was accomplished by bubbling the gas through the reduced-sample solution for several minutes ( $\sim 200$  mL of gas). Ligation by pyridine, pyr (Aldrich, distilled from  $\text{KOH}/\text{CaO}$ ), was accomplished by adding approximately 100 equiv to the solution.<sup>8</sup>

X-band EPR spectra were recorded at 77 K on a Varian E-4 spectrometer. RR spectra were acquired in a 90° scattering configuration on a Spex Industries 1403 double monochromator equipped with a photon-counting detection system and a Hamamatsu R928P photomultiplier tube. Excitation was provided by the discrete outputs of either a Coherent INNOVA-15UV Ar ion or a Coherent K-2000 Kr ion laser. Typical power levels at the sample were 40–50 mW. The spectral slit width was approximately  $5 \text{ cm}^{-1}$ .

## III. Results

**A. Absorption Spectra.** The absorption spectra of the  $[\text{Fe-P}]^-$  complexes are shown in Figure 2. The successive red shift of the Soret maximum reflects the extent of stabilization of the porphyrin  $\pi$  system and parallels the order of the  $[\text{Fe-P}]/[\text{Fe-P}]^-$  redox couples. All of the complexes exhibit low-intensity, split Soret bands and multiple bands in the visible region. The appearance of the absorption spectra of the reduced species has been used previously as prima-facie evidence for porphyrin-centered reduction in these complexes.<sup>9</sup> However, it is important to note that the  $\pi\pi^*$  transitions of the porphyrin (B and Q bands) reflect the *difference* in the properties of the ground and excited electronic states rather than being a measure of the ground-state properties alone. As a consequence, the appearance of the optical spectrum is not necessarily indicative of the electron distribution in the ground state.

The room temperature optical spectra of  $[\text{FeTPP}]^-$  and  $[\text{FeTPPBr}_4]^-$  in the presence of CO and pyridine were examined. It

(19) Spiro, T. G. In *Iron Porphyrins*, Lever, A. B. P., Gray, H. B., Eds.; Addison-Wesley: Reading, MA, 1983; Vol. II, pp 89–159.

(20) (a) Callot, H. J. *Tetrahedron Lett.* **1973**, *50*, 4987–4990. (b) Callot, H. J. *Bull. Soc. Chim. Fr.* **1974**, 1492–1496.

(21) Callot, H. J.; Giraudeau, A.; Gross, M. *J. Chem. Soc. Perkin Trans 2* **1975**, 1321–1324.

(22) (a) Dolphin, D.; Sams, J. R.; Tsui, T. B.; Wong, K. L. *J. Am. Chem. Soc.* **1976**, *98*, 6970–6975. (b) Furhop, J.-H.; Smith, K. M. In *Porphyrins and Metalloporphyrins*; Smith, K. M., Ed.; Elsevier: Amsterdam, 1975; p 798.

(23) Donohoe, R. J. Ph.D. Thesis, North Carolina State University, 1985.

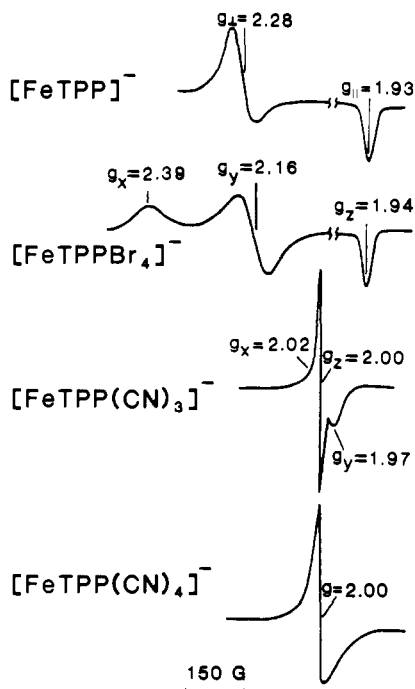


**Figure 3.** Low-temperature (77 K) X-band EPR spectra of the [Fe-P]<sup>-</sup> complexes in DMF, 0.1 M TBAP. Concentrations were approximately  $1 \times 10^{-3}$  M. Typical microwave power was 10 mW and typical modulation amplitude was 8 G.

was found that the spectra in the presence of these ligands are identical with those in their absence. These observations are consistent with previous reports that axial ligands do not bind to [FeTPP]<sup>-</sup> at room temperature.<sup>8,9,14</sup> However, both of these ligands do bind at low temperature (see below).

**B. EPR Spectra.** The low-temperature (77 K) X-band EPR spectra of the [Fe-P]<sup>-</sup> complexes are displayed in Figure 3. The spectra of the complexes are quite distinct. The signal for [FeTPP]<sup>-</sup> is anisotropic and characteristic of an axially symmetric spin system ( $g_{\perp} = 2.28$  and  $g_{\parallel} = 1.93$ ) while the signal for [FeTPPBr<sub>4</sub>]<sup>-</sup> exhibits substantial rhombicity ( $g_x = 2.39$ ,  $g_y = 2.16$ , and  $g_z = 1.94$ ). The EPR signal for [FeTPP(CN)<sub>3</sub>]<sup>-</sup> is collapsed but exhibits a slight anisotropy ( $g_x = 2.02$ ,  $g_z = 2.00$ , and  $g_y = 1.97$ ; these  $g$  values were obtained via simulation of the spectrum; the  $x$ ,  $y$ , and  $z$  assignments are tentative but would be consistent with a small amount of unpaired spin density in a  $d_{\pi}$  orbital). The EPR signal for [FeTPP(CN)<sub>4</sub>]<sup>-</sup> is nearly isotropic and centered at  $g = 2.00$ . The breadth of this signal (25 G) is the result of a slight residual unresolved anisotropy. [It should be noted that the EPR spectrum we obtained for [FeTPP(CN)<sub>4</sub>]<sup>-</sup> in DMF ( $g = 2.03$ , 2.00, 1.98) in which CH<sub>2</sub>Cl<sub>2</sub> was used as the solvent.<sup>17</sup>] The  $g$  values for the various reduced complexes are summarized in Table II.

The addition of pyridine or CO to solutions of [FeTPP]<sup>-</sup> alters the low-temperature EPR spectrum as shown in Figure 4 (see also Table II). It has been previously shown that a single pyridine molecule binds to the reduced complex at low temperature and causes a shift of  $g_{\perp}$  from 2.28 to 2.19.<sup>8</sup> The  $g_{\parallel}$  signal is unshifted but exhibits superhyperfine structure attributable to the interaction of the <sup>14</sup>N nucleus with an unpaired electron in the  $d_{z^2}$  orbital. The addition of CO results in a more dramatic change in the EPR spectrum than does the addition of pyridine. The EPR signal of [FeTPP]<sup>-</sup>·CO is rhombic ( $g_x = 2.01$ ,  $g_z = 2.00$ , and  $g_y = 1.90$ ), and it is reminiscent of that observed for the isoelectronic nitrosyl-ferrochrome complexes ([Fe<sup>II</sup>-P]·NO).<sup>24</sup> Upon incorporation of <sup>57</sup>Fe, the  $g = 2.00$  signal broadens by 3 G, indicating that the  $x$ ,  $y$ , and  $z$  assignments of the  $g$  values are as given in Figure 4.

**Table II.** The  $g$  Values for the [Fe-P]<sup>-</sup> and [Fe-P]<sup>-</sup>·L (L = Pyridine and CO) Complexes Examined in This Study

complex	$g_x$	$g_y$	$g_z$
[FeTPP] <sup>-</sup>	2.28 <sup>a</sup>		1.93
[FeTPP] <sup>-</sup> ·pyr	2.19 <sup>a</sup>		1.93 <sup>d</sup>
[FeTPP] <sup>-</sup> ·CO	2.01	1.90	2.00
[FeTPPBr <sub>4</sub> ] <sup>-</sup>	2.39	2.16	1.94
[FeTPPBr <sub>4</sub> ] <sup>-</sup> ·pyr	2.28	2.12	1.94 <sup>e</sup>
[FeTPPBr <sub>4</sub> ] <sup>-</sup> ·CO	2.01	1.95	2.00
[FeTPP(CN) <sub>3</sub> ] <sup>-</sup>	2.02 <sup>b</sup>	1.97	2.00
[FeTPP(CN) <sub>4</sub> ] <sup>-</sup>		2.00 <sup>c</sup>	

<sup>a</sup> Axially symmetric. <sup>b</sup> The  $x$ ,  $y$ , and  $z$  assignments for this complex are tentative. <sup>c</sup> Isotropic. <sup>d</sup>  $A_{\perp} = 12.5$  G. <sup>e</sup>  $A_z = 11.0$  G.

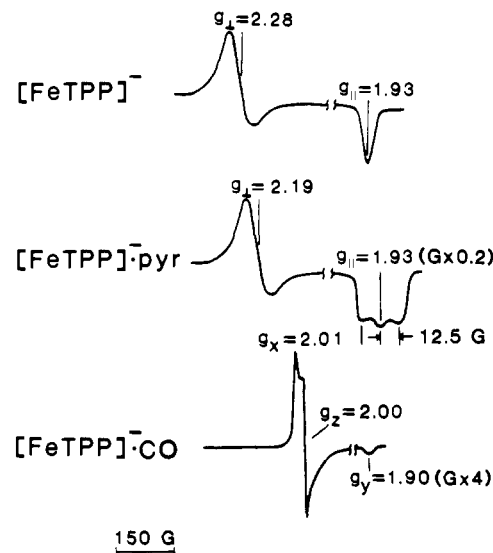


**Figure 4.** Low-temperature (77 K) EPR spectra of [FeTPP]<sup>-</sup> (top), [FeTPP]<sup>-</sup>·pyridine (middle), and [FeTPP]<sup>-</sup>·CO (bottom) in DMF, 0.1 M TBAP. See legend of Figure 3 for experimental details.

This ordering of the  $g$  values is the same as that of nitrosyl-ferrochrome complexes. The similarity of the EPR spectra of [FeTPP]<sup>-</sup>·CO and [Fe<sup>II</sup>-P]·NO suggests that, as is the case for NO, CO is bound in a nonlinear fashion.

The binding of pyridine or CO to [FeTPPBr<sub>4</sub>]<sup>-</sup> alters the EPR spectrum (not shown) of this complex in a fashion similar to that observed for [FeTPP]<sup>-</sup>. For [FeTPPBr<sub>4</sub>]<sup>-</sup>·pyr, the rhombic signal is preserved but the  $g_x$  and  $g_y$  values are collapsed toward  $g = 2$  relative to the unligated complex (see Table II). <sup>14</sup>N-superhyperfine structure is observed on the  $g_z$  component, but the splitting (11 G) is smaller than that observed for [FeTPP]<sup>-</sup>·pyr (12.5 G). In addition, the  $g_x$  and  $g_y$  components of [FeTPPBr<sub>4</sub>]<sup>-</sup>·pyr are observably broadened relative to the analogous  $g$  values of the unligated bromo complex. This broadening may be indicative of unresolved superhyperfine structure on these components. In this regard, broadening of  $g_{\perp}$  is not observed upon binding of pyridine to [FeTPP]<sup>-</sup>.

**C. RR Spectra.** The high-frequency portion of the B-state-excitation RR spectrum of [FeTPP]<sup>-</sup> is shown in Figure 5 (bottom). For comparison, the spectra of the unreduced, high-spin (top) and low-spin (middle) complexes are also displayed. The spectrum we report here for [FeTPP]<sup>-</sup> was obtained with  $\lambda_{ex} = 457.9$  nm whereas the spectrum we previously reported for this complex was obtained with  $\lambda_{ex} = 413.1$  nm.<sup>8</sup> We have now determined that the RR features observed with 413.1-nm excitation are predominantly due to scattering from small amounts of residual unreduced material. This scattering predominates at  $\lambda_{ex} = 413.1$  nm because the extinction coefficient of FeTPP is significantly greater than that of [FeTPP]<sup>-</sup> at this wavelength. In contrast, at 457.9 nm the extinction coefficient of the latter species is much larger than that of the former. It should also be noted that the reduced complexes in general exhibit poor RR scattering due to their extremely broad absorption bands. As a consequence, extreme care was taken to find the optimal wave-

(24) Palmer, G. In *The Porphyrins*; Dolphin, D., Ed.; Academic: New York, 1978; Vol. IV, pp 313-353.

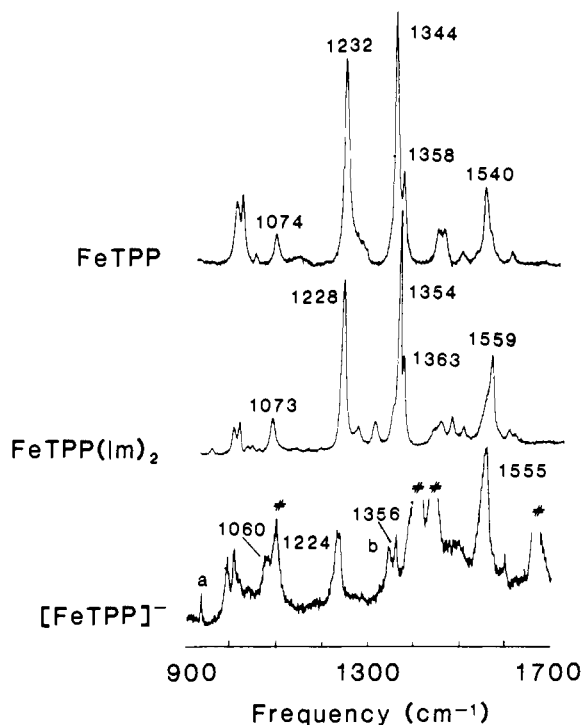


**Figure 5.** Resonance Raman spectra of high-spin  $\text{Fe}^{\text{II}}\text{TPP}$  [ $\lambda_{\text{ex}} = 413.1$  nm (top)], low-spin  $\text{Fe}^{\text{II}}\text{TPP}$  [ $\lambda_{\text{ex}} = 413.1$  nm (middle)], and  $[\text{Fe}^{\text{I}}\text{TPP}]^-$  [ $\lambda_{\text{ex}} = 457.9$  nm (bottom)] in DMF, 0.1 M TBAP. Peak a is due to TBAP. Peak b is due to  $\text{Fe}^{\text{II}}\text{TPP}$ . Solvent modes are denoted by #. Typical concentrations ranged from  $1 \times 10^{-4}$  ( $\text{Fe}^{\text{II}}\text{-P}$ ) to  $1 \times 10^{-3}$  M ( $[\text{Fe-P}]^-$ ).

lengths for the RR experiments. Nevertheless, some of the RR spectra exhibit features due to unreduced material even at the optimal wavelength for scattering from the reduced products.

Reduction of the high-spin  $\text{Fe}^{\text{II}}\text{TPP}$  complex results in upshifts of the two strong polarized RR bands at 1344 and 1540  $\text{cm}^{-1}$  to 1356 and 1555  $\text{cm}^{-1}$ , respectively (cf. Figure 5, top and bottom). For convenience, we retain the nomenclature traditionally used for octaalkylporphyrins and refer to these modes as  $\nu_4$  and  $\nu_2$ , respectively.<sup>15</sup> However, the compositions of the normal modes of tetraarylporphyrins are significantly different from those of octaalkylporphyrins; hence, the spin- and oxidation-state sensitivities of these two RR bands are quite different for the two types of porphyrins.<sup>25</sup> In this connection, previous RR studies of  $\text{Fe}^{\text{II}}\text{TPP}$  have shown that both the  $\nu_2$  and  $\nu_4$  modes undergo large upshifts upon conversion of the  $\text{Fe}^{\text{II}}$  ion from high to low spin (cf. Figure 5, top and middle).<sup>25</sup> Examination of Figure 5 reveals that the  $\nu_4$  band of  $[\text{Fe}^{\text{I}}\text{TPP}]^-$  occurs at approximately the same frequency as the analogous band of low-spin  $\text{Fe}^{\text{II}}\text{TPP}$  (1356 vs. 1354  $\text{cm}^{-1}$ ) whereas the  $\nu_2$  band is slightly downshifted (1555 vs. 1559  $\text{cm}^{-1}$ ). These data are summarized in Table III.

The frequencies of  $\nu_4$  and  $\nu_2$  observed for  $[\text{Fe}^{\text{I}}\text{TPP}]^-$  indicate a low-spin formulation for the metal center at room temperature, which is consistent with magnetic measurements.<sup>9,12</sup> On the other hand, it was concluded in a recent RR study<sup>13</sup> that the  $[\text{FeOEP}]^-$  complex has a high-spin metal center at room temperature. However, this conclusion is incompatible with both the room-temperature  $^2\text{H}$  paramagnetic shifts and magnetic moment determined for this complex by Hickman et al.<sup>12</sup> We have confirmed the results of this latter study via  $^1\text{H}$  NMR measurements which indicate that the  $[\text{Fe-P}]^-$  complexes exhibit a low-spin configuration at room temperature in both DMF and tetrahydrofuran. In that the magnetic moment provides a far more definitive indication of spin state than does the vibrational spectrum, we conclude that the high-spin formulation advanced by Teraoka et al.<sup>13</sup> is incorrect.

**Table III.** Raman Frequencies ( $\text{cm}^{-1}$ ) of  $\nu_4$  and  $\nu_2$  for High-Spin (hs)  $\text{Fe}^{\text{II}}\text{-P}$ , Low-Spin (ls)  $\text{Fe}^{\text{II}}\text{-P}$ ,  $[\text{Fe-P}]^-$ ,  $\text{M-P}$ , and  $[\text{M-P}]^-$  Complexes in DMF

porphyrin (P)		$\text{Fe}^{\text{II}}\text{-P}$ (hs)	$\text{Fe}^{\text{II}}\text{-P}$ (ls)	$[\text{Fe-P}]^-$	$\text{M-P}^a$	$[\text{M-P}]^-$
TPP	$\nu_4$	1344	1354	1356	1351	1346
	$\nu_2$	1540	1559	1554	1548	1531
$\text{TPPBr}_4$	$\nu_4$	1337	1344	1342	<i>b</i>	<i>c</i>
	$\nu_2$	1532	1544	1536		
$\text{TPP}(\text{CN})_3$	$\nu_4$	1347	1361	1360	1357	1358
	$\nu_2$	1546	1556	1536	1549	<i>d</i>
$\text{TPP}(\text{CN})_4$	$\nu_4$	1346	1361	1360	1368	1371
	$\nu_2$	1542	1557	1535	1570	<i>d</i>

<sup>a</sup>  $\text{M} = \text{Cu}$  for  $\text{MTPP}(\text{CN})_4$  and  $[\text{MTPP}(\text{CN})_4]^-$ , otherwise  $\text{M} = \text{Zn}$ .  
<sup>b</sup> The  $\text{ZnTPPBr}_4$  complex is photolyzed by laser irradiation. <sup>c</sup> The  $[\text{ZnTPPBr}_4]^-$  complex is not chemically stable (see text). <sup>d</sup> These frequencies could not be reliably identified (see text).

In order to examine the effects of macrocycle-centered reduction, we obtained RR spectra of  $\text{ZnTPP}$  and  $[\text{ZnTPP}]^-$ . Ksenofontova et al.<sup>26</sup> and Yamaguchi et al.<sup>27</sup> have previously reported RR spectra for  $[\text{ZnTPP}]^-$ ; however, the results are not in agreement. Our results are consistent with those of the former study and show that the  $\nu_4$  band is relatively insensitive to macrocycle-centered reduction whereas the  $\nu_2$  band undergoes a substantial downshift (17  $\text{cm}^{-1}$ ) (see Table III). The shifts observed for  $\nu_4$  and  $\nu_2$  are not readily interpretable on the basis of the atomic electron densities predicted for the  $e_g^*$  orbitals.<sup>19</sup> On the basis of these densities, one might predict that both  $\nu_4$  and  $\nu_2$  should downshift upon reduction with  $\nu_4$  exhibiting the larger shift. In that such behavior is not observed for either  $\text{ZnTPP}$  or the  $\beta$ -alkyl-substituted Zn etioporphyrin complex (in which  $\Delta\nu_4 = -7$   $\text{cm}^{-1}$  and  $\Delta\nu_2 = -23$   $\text{cm}^{-1}$ ),<sup>26</sup> it is clear that it is not possible to predict the frequency shifts on the basis of the simple orbital diagram alone.

The RR data for  $[\text{ZnTPP}]^-$  suggest that if reduction of  $\text{Fe}^{\text{II}}\text{TPP}$  is predominantly ring-centered then  $\nu_2$  would be found at a substantially lower frequency than is observed for low-spin  $\text{Fe}^{\text{II}}\text{TPP}$ . Conversely, if the reduction is predominantly metal-centered,  $\nu_2$  for  $[\text{Fe}^{\text{I}}\text{TPP}]^-$  should occur at essentially the same frequency as observed for the low-spin  $\text{Fe}^{\text{II}}$  complex. This latter conclusion is based on analogy to the behavior of  $\nu_2$  upon reduction of low-spin  $\text{Co}^{\text{III}}$  porphyrins in which the addition of the electron to the  $d_{z^2}$  orbital does not significantly perturb the vibrational frequencies of the macrocycle.<sup>28,29</sup> The behavior of  $\nu_2$  upon reduction of  $\text{Fe}^{\text{II}}\text{TPP}$  is clearly more consistent with predominantly metal-centered rather than ring-centered reduction.

The frequencies of the  $\nu_4$  and  $\nu_2$  bands of the Fe complexes of  $\text{TPPBr}_4$  are summarized in Table III. The upshift of  $\nu_4$  upon reduction is again indicative of a spin-state change. The behavior of  $\nu_2$  upon generation of  $[\text{Fe}^{\text{I}}\text{TPPBr}_4]^-$  is similar to that observed upon generation of  $[\text{Fe}^{\text{I}}\text{TPP}]^-$ ; that is, the frequency of  $\nu_2$  falls between that found in the high- and low-spin unreduced complexes. However, the downshift for this mode in the reduced bromo complex relative to the low-spin analogue (8  $\text{cm}^{-1}$ ) is larger than that observed for  $\text{Fe}^{\text{II}}\text{TPP}$  (4  $\text{cm}^{-1}$ ). This could reflect different electron distributions in the two reduced complexes. On the other hand, it should be noted that the frequencies of  $\nu_2$  and  $\nu_4$  for  $\text{Fe}^{\text{II}}\text{TPPBr}_4$  are different from those of  $\text{Fe}^{\text{II}}\text{TPP}$  (as well as those of the two cyano derivatives; see below) and undergo different shifts upon spin-state conversion than do these other complexes. This is presumably due to a change in the composition of the normal modes which occurs as a result of the heavy bromine atoms at the periphery of the ring. Unfortunately, we were unable to determine the effects of a purely macrocycle-centered reduction

(26) Ksenofontova, N. M.; Maslov, V. G.; Sidorov, A. N.; Bobovich, Ya. S. *Opt. Spectrosc.* **1976**, *40*, 462-465.

(27) Yamaguchi, H.; Soeta, A.; Toeda, H.; Itoh, K. *J. Electroanal. Chem.* **1983**, *159*, 347-359.

(28) Woodruff, W. H.; Adams, D. H.; Spiro, T. G.; Yonetani, T. *J. Am. Chem. Soc.* **1975**, *97*, 1695-1698.

(29) Spaulding, L. D.; Chang, C. C.; Yu, N.-T.; Felton, R. H. *J. Am. Chem. Soc.* **1975**, *97*, 2517-2525.

(25) Burke, J. M.; Kincaid, J. R.; Peters, S.; Gagne, R. R.; Collman, J. P.; Spiro, T. G. *J. Am. Chem. Soc.* **1978**, *100*, 6083-6088.

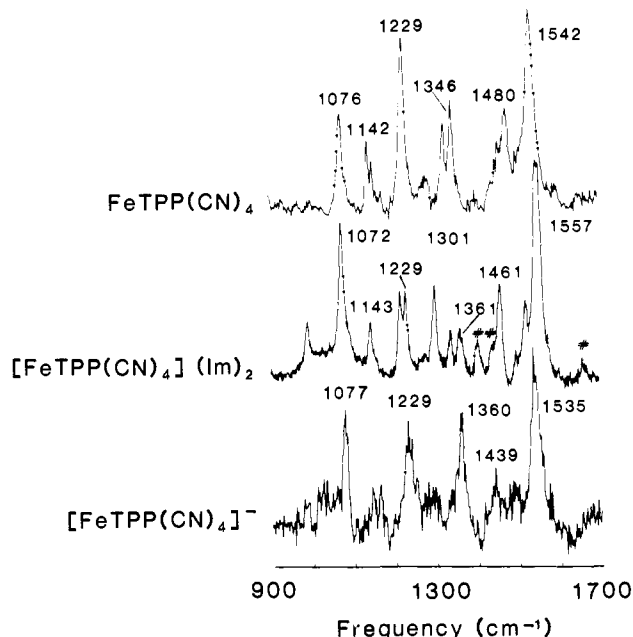


**Figure 6.** Resonance Raman spectra of high-spin  $\text{Fe}^{\text{II}}\text{TPP}(\text{CN})_4$  [ $\lambda_{\text{ex}} = 457.9$  nm (top)], low-spin  $\text{Fe}^{\text{II}}\text{TPP}(\text{CN})_4$  [ $\lambda_{\text{ex}} = 457.9$  nm (middle)], and  $[\text{FeTPP}(\text{CN})_4]^-$  [ $\lambda_{\text{ex}} = 476.5$  nm (bottom)] in DMF, 0.1 M TBAP. Solvent modes are denoted by #. Typical concentrations ranged from  $1 \times 10^{-4}$  ( $\text{Fe}^{\text{II}}\text{-P}$ ) to  $1 \times 10^{-3}$  M ( $[\text{Fe-P}]^-$ ).

on the RR spectra of the  $\text{TPPBr}_4$  moiety because  $[\text{ZnTPPBr}_4]^-$  (as well as  $[\text{H}_2\text{TPPBr}_4]^-$ ) is chemically unstable.

The high-frequency portion of the B-state-excitation RR spectra of  $[\text{FeTPP}(\text{CN})_4]^-$  is shown in Figure 6. For comparison, the spectra of the analogous unreduced high-spin and low-spin complexes are also shown. The RR data for the various  $\text{FeTPP}(\text{CN})_3$  complexes are essentially identical with those of the tetracyano analogues. The pertinent RR data for the cyano complexes are summarized in Table III. The  $\nu_4$  bands of the reduced cyano complexes occur at frequencies similar to those of the  $\nu_4$  bands of the low-spin  $\text{Fe}^{\text{II}}$  analogues, which is consistent with a change in spin state upon reduction. The  $\nu_2$  bands in the reduced cyano complexes are significantly downshifted ( $\sim 20$   $\text{cm}^{-1}$ ) from those observed in the low-spin  $\text{Fe}^{\text{II}}$  analogues. This frequency difference is similar in magnitude to the shift observed for the corresponding mode of  $\text{ZnTPP}$  upon reduction (17  $\text{cm}^{-1}$ ). Thus, the RR results in conjunction with the EPR data for  $[\text{FeTPP}(\text{CN})_3]^-$  and  $[\text{FeTPP}(\text{CN})_4]^-$  indicate that these complexes are primarily  $\pi$ -anion radical in character.

In order to explore the effects of a macrocycle-centered reduction on the  $\text{TPP}(\text{CN})_3$  and  $\text{TPP}(\text{CN})_4$  ligands, we acquired the RR data for the reduced and unreduced Zn complexes of these moieties. For the latter ligand, satisfactory spectra could not be obtained due to impurities; therefore, the Cu complex was examined. The RR data for reduced and unreduced  $\text{ZnTPP}(\text{CN})_3$  and  $\text{CuTPP}(\text{CN})_4$  are given in Table III. The  $\nu_4$  bands of these complexes do not shift upon reduction as is the case for the analogous mode of  $\text{ZnTPP}$ . The behavior of  $\nu_2$  could not be determined with certainty for either of the metalocyanoporphyrins due to the complicated band pattern in this spectral region. Nevertheless, we conclude that the normal-mode descriptions for the  $\nu_4$  and  $\nu_2$  vibrations of  $\text{FeTPP}(\text{CN})_4$  and  $\text{FeTPP}(\text{CN})_3$  are similar to those of the analogous modes of  $\text{FeTPP}$ . This conclusion is substantiated by the fact that spin-state conversion results in identical frequency shifts of the  $\nu_4$  modes of the three different  $\text{Fe}^{\text{II}}\text{-P}$  complexes as well as identical shifts of the  $\nu_2$  modes.

#### IV. Discussion

**A. Effects of Altering Porphyrin Orbital Energies.** In order to discuss the nature of the electronic structure of the  $[\text{Fe-P}]^-$  complexes, it is crucial to distinguish between the amount of paired and unpaired electron density in the metal  $d_\pi$  and  $d_{z^2}$  and the porphyrin  $e_g^*$  orbitals. The limiting-case  $d^7 \text{Fe}^{\text{I}}$  and  $\text{Fe}^{\text{II}} \pi$ -an-

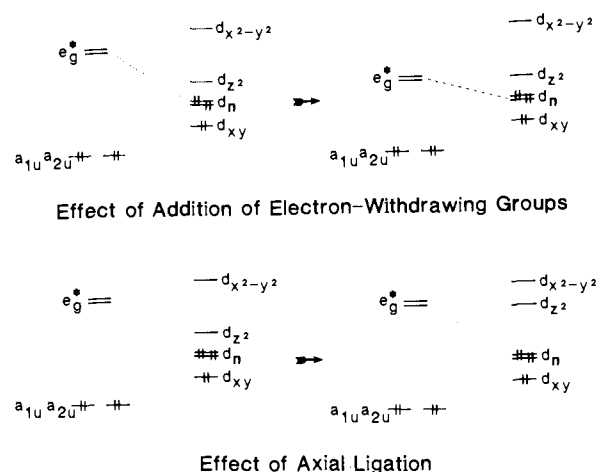


**Figure 7.** Orbital energy diagram for low-spin  $\text{Fe}^{\text{II}}$  porphyrins. The effects of electron-withdrawing groups on the porphyrin orbitals are illustrated in the top panel while the effects of axial ligands on the metal orbitals are illustrated in the bottom panel.

ion-radical configurations which have often been invoked to represent the distribution of electrons in the reduced systems do not lend themselves toward making this distinction. The difficulties associated with a limiting-case description for the one-electron reduction products were recognized by Reed,<sup>9</sup> who suggested that both forms contribute to the electronic configuration of  $[\text{FeTPP}]^-$ . Reed proposed a resonance scheme in which the unpaired electron was shared between the porphyrin  $e_g^*$  and metal  $d_\pi$  orbitals. The  $S = 1/2$  properties indicated by the magnetic data were rationalized by invoking antiferromagnetic coupling between the unpaired electron on the macrocycle and an  $S = 1$   $\text{Fe}^{\text{II}}$  ion. However, subsequent NMR measurements showed that the unpaired electron resides in the metal  $d_{z^2}$  orbital rather than the  $\pi$  molecular orbitals.<sup>12</sup> This result invalidates resonance wherein unpaired electron density is shared between the metal and porphyrin  $\pi$  orbitals. Nevertheless, the symmetry equivalence of these orbitals does allow the sharing of paired electron density (back-bonding). Indeed, the sharing of paired density is important even in unreduced low-spin  $\text{Fe}^{\text{II}}\text{-P}$  complexes where it can be estimated that each of the "metal"  $\pi$  orbitals is actually 90% metal and 10% ligand in character.<sup>30,31</sup> For the  $\beta$ -pyrrole-substituted derivatives examined in this study, these orbitals may in fact contain a greater contribution from the ligand due to lowering of the  $e_g^*$  orbital energies as is shown schematically in Figure 7 (top). The mixing of the metal and porphyrin  $\pi$  orbitals dictates that reduction must to some extent affect the energies and spatial descriptions of both sets of orbitals.

Although the magnetic data reported for  $[\text{FeTPP}]^-$  demonstrate that the unpaired electron density resides in the  $d_{z^2}$  orbital ( $^2A_{1g}$  ground state), these data do not allow the assessment of the extent of paired density which has been transferred from the metal to the porphyrin  $\pi$  orbitals via back-bonding. On the other hand, the RR frequencies are quite sensitive to the extent of back-bonding.<sup>19</sup> To a first approximation, the addition of unpaired electron density to the porphyrin  $e_g^*$  orbitals should alter the vibrational frequencies of the macrocycle in a manner similar to that caused by the transfer of an equivalent amount of paired electron density. The  $\nu_2$  mode is observed to be especially sensitive to changes in the amount of electron density on the macrocycle. Thus, the 4- $\text{cm}^{-1}$  difference between the frequencies of this band for low-spin  $\text{Fe}^{\text{II}}\text{TPP}$  and  $[\text{FeTPP}]^-$  suggests that some amount of paired electron density is transferred to the macrocycle upon reduction. The delocalization of additional charge onto the ring is intuitively appealing because this process provides a means of stabilizing the negatively charged metal ion. If it is assumed that

(30) Lin, W. C. In *The Porphyrins*; Dolphin, D., Ed.; Academic: New York, 1978; Vol. IV, pp 355-377.

(31) Loew, G. H. In *Iron Porphyrins*; Lever, A. P. B., Gray, H. B., Eds.; Addison-Wesley: Reading, MA, 1983; Vol. I, pp 1-87.

the 17-cm<sup>-1</sup> shift that occurs upon reduction of ZnTPP to [ZnTPP]<sup>-</sup> represents the effect of addition of one electron to the macrocycle, we may roughly estimate that 4 cm<sup>-1</sup> represents the addition of paired electron density equivalent to approximately 1/4 of an electron. Thus, while the unpaired electron in [FeTPP]<sup>-</sup> resides in a purely metal-centered orbital (d<sub>z<sup>2</sup></sub>), paired-electron density in the porphyrin e<sub>g</sub>\* orbitals has been substantially increased relative to that present in the Fe<sup>II</sup>TPP complex.

The general features of the EPR spectrum of [FeTPPBr<sub>4</sub>]<sup>-</sup> indicate that, as is the case for [FeTPP]<sup>-</sup>, the unpaired electron resides in the d<sub>z<sup>2</sup></sub> orbital (<sup>2</sup>A<sub>1g</sub> ground state). However, the large rhombicity in the EPR signal for the bromo complex implies that the <sup>2</sup>E<sub>g</sub> excited state of the metal that arises from a (d<sub>π</sub>)<sup>3</sup> configuration is split. This excited state is the primary contributor to g<sub>⊥</sub>.<sup>30,32,33</sup> It should be noted that the EPR spectrum of high-spin Fe<sup>III</sup>TPPBr<sub>4</sub>Cl is axially symmetric, which indicates that the ligand alone is not the source of this splitting. The splitting of the <sup>2</sup>E<sub>g</sub> excited state of the metal ion in [FeTPPBr<sub>4</sub>]<sup>-</sup> can be rationalized as follows. The stabilization of the porphyrin e<sub>g</sub>\* orbitals by the bromo substituents increases the mixing of the porphyrin and metal π orbitals relative to that which is present in FeTPP (see Figure 7, top). As a consequence, the wave function for the "metal-like" <sup>2</sup>E<sub>g</sub> excited state acquires more ligand character. The delocalization of the unpaired electron onto the ligand allows stabilization of this excited state via a Jahn-Teller distortion. This distortion breaks the degeneracy of the excited state and results in a rhombic EPR signal.

The RR spectra show that the ν<sub>2</sub> band of [FeTPPBr<sub>4</sub>]<sup>-</sup> is 8 cm<sup>-1</sup> lower in frequency than the analogous mode of the low-spin Fe<sup>II</sup> parent complex. Ideally, it would be desirable to compare this frequency difference to that observed upon exclusively macrocycle-centered reduction of the TPPBr<sub>4</sub> moiety. However, as was noted in the Experimental Section, the [ZnTPPBr<sub>4</sub>]<sup>-</sup> complex is unstable and we were unable to obtain RR data for this material. If the 8-cm<sup>-1</sup> frequency difference observed for the bromo complexes can be directly compared to the 4-cm<sup>-1</sup> difference observed for FeTPP, it can be estimated that transfer of paired electron density to the TPPBr<sub>4</sub> macrocycle via back-bonding is approximately twice as large as in the unsubstituted complex. This increased interaction between the metal and porphyrin π orbitals in the <sup>2</sup>A<sub>1g</sub> ground state is consistent with the increased mixing in the <sup>2</sup>E<sub>g</sub> excited state as is manifested in the EPR spectrum.

The spectral data for [FeTPP(CN)<sub>3</sub>]<sup>-</sup> and [FeTPP(CN)<sub>4</sub>]<sup>-</sup> indicate that an unpaired electron resides on the macrocycle. The extremely small anisotropy observed for the EPR signals of the two reduced cyano complexes precludes the unlikely possibility that the unpaired electron resides in the d<sub>z<sup>2</sup></sub> orbital while paired electron density equivalent to one electron is transferred to the ring. Nevertheless, the slight anisotropy does indicate that some unpaired electron density resides on the metal. The origin of this unpaired electron density is not immediately obvious. There are a number of possibilities for the ground electronic state of a reduced complex in which an unpaired electron resides on the macrocycle. If the Fe<sup>II</sup> ion is in a low-spin configuration, as is suggested by our RR results, the ground state would be <sup>2</sup>E<sub>g</sub>. On the other hand, if the metal ion is in an intermediate- or high-spin configuration, a number of other possibilities exist. The high-spin configuration can be immediately excluded on the basis of the magnetic data.<sup>9,12</sup> As will now be discussed, the magnetic data as well as the RR data also exclude the intermediate-spin configuration for the metal ion.

As previously noted, the upshift in the ν<sub>4</sub> band that occurs for the cyano complexes upon reduction indicates that the spin state of the metal ion has changed. The frequency of the ν<sub>4</sub> band in the reduced complexes is essentially identical with that observed for the low-spin, unreduced complexes and is substantially lower in frequency than is expected for intermediate-spin Fe<sup>II</sup>-P systems.<sup>25</sup> Because ν<sub>4</sub> is insensitive to reduction of the macrocycle (see Table III), its frequency in the two reduced cyano complexes

suggests a low-spin configuration for the metal ion. The nearly isotropic EPR spectra observed for the reduced cyano-substituted complexes are also consistent with the low-spin configuration for the Fe<sup>II</sup> ion. To obtain such a spectrum from an S = 1/2 ground state which arises from antiferromagnetic coupling between an intermediate-spin, S = 1, Fe<sup>II</sup> center and an S = 1/2 porphyrin radical would require that the exchange interaction be negligible relative to the zero-field splitting of the metal ion.<sup>34-36</sup> However, negligible coupling is implausible due to the direct overlap of the d<sub>π</sub> and e<sub>g</sub>\* orbitals. Reduction of the macrocycle apparently results in a change in its geometry such that a low-spin configuration is preferred for the metal ion. A filled metal t<sub>2g</sub> subshell in conjunction with an unpaired electron in the porphyrin e<sub>g</sub>\* orbitals leads to a <sup>2</sup>E<sub>g</sub> ground state for the complex. Nevertheless, the residual anisotropy in the EPR spectra of the reduced cyano complexes indicates that the wave function for the unpaired electron does contain a small amount of metal d<sub>π</sub> character. Thus, metal/porphyrin π-orbital interaction is relevant even in the macrocycle-reduced complexes.

**B. Effects of Altering Metal Orbital Energies.** The primary effect of axial ligation is to destabilize the metal d<sub>z<sup>2</sup></sub> orbital relative to the d<sub>π</sub> orbitals as is shown in Figure 7 (bottom). This perturbation is directly manifested in the value of g<sub>⊥</sub>. Ligation of pyridine to [FeTPP]<sup>-</sup> shifts g<sub>⊥</sub> from 2.28 to 2.19 while ligation to [FeTPPBr<sub>4</sub>]<sup>-</sup> shifts g<sub>x</sub> from 2.39 to 2.28 and g<sub>y</sub> from 2.16 to 2.12 (see Table II). The appearance of these EPR spectra clearly indicates that, despite destabilization, the unpaired electron remains in the d<sub>z<sup>2</sup></sub> orbital and the <sup>2</sup>A<sub>1g</sub> ground states are retained. In the case of [FeTPPBr<sub>4</sub>]<sup>-</sup>-pyr, the <sup>14</sup>N superhyperfine splittings are different from those of [FeTPP]<sup>-</sup>-pyr. This result may be due to the different degrees of ligand character in the excited states of the two complexes. Changes in the character of the "metal-like" <sup>2</sup>E<sub>g</sub> excited state would alter the indirect dipolar contributions to the hyperfine interactions.

It is of interest to compare the EPR spectra of [FeTPP]<sup>-</sup> in the presence and absence of pyridine to the EPR data for the isoelectronic Co<sup>II</sup>TPP complex under similar conditions.<sup>30,32,33</sup> Upon ligation of a single pyridine to four-coordinate Co<sup>II</sup>TPP, the value of g<sub>⊥</sub> shifts from 3.32 to 2.33, substantially more than the shift observed for [FeTPP]<sup>-</sup>. The smaller shift in the iron complex could reflect a lower affinity for a pyridine ligand. An alternative explanation is that [FeTPP]<sup>-</sup> binds a DMF molecule at low temperature and that pyridine displaces this ligand. In this regard, the absolute value of g<sub>⊥</sub> for [FeTPP]<sup>-</sup> (2.28) is more consistent with the g<sub>⊥</sub> value of five-coordinate Co<sup>II</sup>TPP (2.33).

The anisotropy in the EPR spectra of [FeTPP]<sup>-</sup>-CO and [FeTPPBr<sub>4</sub>]<sup>-</sup>-CO suggests that the unpaired electron resides in a metal-like orbital. However, the anisotropy is substantially smaller than that observed for the unligated complexes or the pyridine adducts. The collapsed appearance of the EPR spectra of the CO adducts is probably due to the partial delocalization of the unpaired electron into a π\* orbital on the CO ligand. The identity of the metal orbital that contains the unpaired electron density is not entirely clear. The anisotropy in the EPR spectrum could result if the electron remains in the d<sub>z<sup>2</sup></sub> orbital (<sup>2</sup>A<sub>1</sub> ground state) and the degeneracy of the d<sub>π</sub> orbitals is removed. This loss of degeneracy is expected because the CO ligand is forced to bind through one of its empty π\* orbitals, which results in a bent geometry. If the rearrangement of the metal orbital energies is sufficiently large, the unpaired electron may reside in a metal orbital that is predominantly d<sub>π</sub> (<sup>2</sup>E ground state) rather than d<sub>z<sup>2</sup></sub> (<sup>2</sup>A<sub>1</sub> ground state). The EPR data for [FeTPP]<sup>-</sup>-CO and [FeTPPBr<sub>4</sub>]<sup>-</sup>-CO are compatible with either a <sup>2</sup>A<sub>1</sub> or a <sup>2</sup>E ground state.<sup>37</sup>

(34) Rutter, R.; Hagar, L. P.; Dhonau, H.; Hendrich, M.; Valentine, M.; Debrunner, P. *Biochemistry* **1984**, *23*, 6809-6816.

(35) Lang, G.; Spartalian, K.; Reed, C. A.; Collman, J. P. *J. Chem. Phys.* **1978**, *69*, 5424-5427.

(36) Mispelter, J.; Momenteau, M.; Lhoste, J. M. *J. Chem. Phys.* **1980**, *72*, 1003-1012.

(37) (a) Trittelvitz, E.; Gersonde, K.; Winterhalter, K. H. *Arch. Biochem. Biophys.* **1974**, *193*, 301-313. (b) Morse, R. H.; Chan, S. I. *J. Biol. Chem.* **1980**, *225*, 7876-7882.

(32) Lin, W. C. *Mol. Phys.* **1976**, *31*, 657-662.

(33) Lin, W. C. *Inorg. Chem.* **1976**, *15*, 1114-1118.

**C. Further Considerations.** Our results indicate that the electron density on the macrocycle is increased for all of the  $[\text{Fe-P}]^-$  complexes relative to the unreduced materials. This increased electron density (paired or unpaired) may account for the geometry of the  $[\text{FeTPP}]^-$  system in the crystalline environment<sup>16</sup> as well as the appearance of the optical spectra of all four reduced complexes. Significant back-donation of paired electron density from the metal to the porphyrin ring could alter the macrocycle geometry in a fashion similar to that which would occur upon ring-centered reduction. Such changes in geometry may alter the form of the normal modes of vibration and lead to the unexpected shifts observed for the  $\nu_2$  and  $\nu_4$  bands. Extensive metal/porphyrin interaction would also be expected to perturb the electronic states involved in the optical transitions. For example, the electron density on the macrocycle may be significantly different in the excited  $\pi\pi^*$  states which give rise to the B and Q absorption bands than in the ground electronic state. Electron density redistribution could result in large origin shifts which would give rise to Franck-Condon progressions not typically observed for the Q and B absorption bands of porphyrins. Furthermore, extensive mixing of the porphyrin and metal  $\pi$  orbitals could enhance the oscillator strength of formally forbidden charge-transfer transitions.<sup>38</sup> Two types of charge-transfer transitions can occur: one which involves single excitations ( $d_\pi \rightarrow e_g^*$ ) and the other which involves double excitations ( $a_{1u}$  or  $a_{2u} \rightarrow e_g^* + d_\pi \rightarrow e_g^*$ ) (see Figure 7). Both types of transitions have been proposed to occur in low-valent metalloporphyrins.<sup>39</sup>

Thus far, only the qualitative features of the EPR spectra have been examined in order to characterize the reduced complexes. A detailed analysis of the  $g$  values supports the earlier conclusion that metal/porphyrin interaction is important. Although the general features of the EPR spectra of  $[\text{FeTPP}]^-$  and  $[\text{FeTPPBr}_4]^-$  clearly indicate a  $d^7 \text{Fe}^1$  configuration, the observed  $g$  values are unusual. In particular,  $g_{\parallel}$  is extremely low (see Figure 3). Values of  $g_{\parallel}$  that are significantly below  $g = 2$  have been observed for  $d^7 \text{Co}^{II}$  porphyrins; however, these systems also exhibit values of  $g_{\perp}$  that are much higher than those observed for the  $[\text{Fe}^I\text{-P}]^-$  complexes.<sup>30,32,33</sup> We attempted to reproduce the observed  $g$  values of  $[\text{FeTPP}]^-$  and  $[\text{FeTPPBr}_4]^-$  by using the basis set that has been successfully employed by Lin to describe the  $g$  values of  $d^7 \text{Co}^{II}$  porphyrins.<sup>33</sup> In this treatment, the wave function for the  $d^7$  ground-state configuration is calculated by diagonalizing the Hamiltonian matrix derived from a 16-function basis set comprised of all symmetry-allowed single- and relevant double-excited-state configurations of the metal ion. The spin-orbit and electrostatic parameters are held constant while the crystal field parameters are adjusted in order to fit the  $g$  values. In our calculation, the values of the spin-orbit parameter,  $\lambda$ ,<sup>40</sup> and electrostatic parameters,  $B$  and  $C$ ,<sup>41</sup> were initially assumed to be those of the  $d^7 \text{Fe}^1$

ion. Calculations with these values as well as calculations with other reasonable estimates for  $\lambda$ ,  $B$ , and  $C$  failed to reproduce the observed  $g$  values for the  $[\text{Fe}^I\text{-P}]^-$  complexes. Attempts were also made to fit the  $g$  values by incorporating orbital reduction in order to account for partial delocalization of the  $d_\pi$  electrons onto the ligand. This effort failed because simple orbital reduction simultaneously influences the values of both  $g_{\perp}$  and  $g_{\parallel}$  such that the observed spectra cannot be reproduced. The results of these calculations suggest that if the delocalization of paired electron density onto the ligand significantly influences the  $g$  values then this delocalization must be accounted for in a more sophisticated fashion than is allowed by orbital reduction. It may also be necessary to consider delocalization of unpaired electron density in order to reproduce the  $g$  values. This type of delocalization would be represented by quantum-mechanically admixing low-lying charge-transfer excited states into the ground-state wave function. At present, insufficient information is available to allow the assessment of the relative importance of the various factors that contribute to the magnetic properties of the  $[\text{Fe}^I\text{-P}]^-$  complexes.

## V. Summary and Conclusions

The spectroscopic results we have reported herein demonstrate that the electron density in singly reduced  $\text{Fe}^{II}$  porphyrins can be systematically transferred between the metal atom and porphyrin ring by altering the electron-withdrawing capability of the porphyrin ligand. For all of the complexes examined, reduction results in a low-spin configuration for the metal ion, regardless of whether the unpaired electron resides on the metal or the ring. Complexes for which the  $[\text{Fe}^{II}\text{-P}]/[\text{Fe}^I\text{-P}]^-$  redox couple is more negative than  $-0.812 \text{ V}$  (vs.  $\text{Ag}/\text{AgCl}$ ) have the unpaired electron in the metal  $d_{z^2}$  orbital which results in a  $^2A_{1g}$  ground state. Systems for which the redox couple is more positive than  $-0.539 \text{ V}$  have the unpaired electron on the macrocycle which results in a  $^2E_g$  ground state. Regardless of the formal ground state of the  $[\text{Fe}^I\text{-P}]^-$  complexes, there is extensive interaction between the metal  $d_\pi$  and porphyrin  $e_g^*$  orbitals. This result is in general, although not specific, agreement with the resonance formulation proposed for these systems by Reed.<sup>9</sup>

The electron distribution observed for the  $[\text{Fe}^I\text{-P}]^-$  complexes relative to their redox potentials suggests that reduction of the heme moieties in redox proteins would probably yield a metal-centered reduction product. In order to attain a  $\pi$ -anion-radical configuration, a heme moiety would have to contain substituents that are not currently thought to be associated with biological iron porphyrins. The very negative reduction potentials characteristic of typical biologically relevant hemes would seemingly preclude the importance of highly reduced species as intermediates in heme redox protein chemistry.

**Acknowledgment.** This work was supported by Grant GM-36243 from the National Institute of General Medical Sciences to D.F.B. The authors are grateful to Dr. C. A. Marrese for expert advice on electrochemical techniques, Professor J. S. Lindsey for the use of the Chromatotron, Dr. G. S. Srivatsa for obtaining the EPR spectrum of  $[\text{FeTPP}]^- \text{-CO}$ , N. J. Boldt for obtaining the Raman spectrum of  $[\text{FeTPP}(\text{CN})_4]^-$ , and Professor K. M. Kadish for the gift of  $\text{FeTPP}(\text{CN})_4\text{Cl}$ . D.F.B. also acknowledges helpful discussions with Professor E. I. Solomon.

(38) Gouterman, M. In *The Porphyrins*; Dolphin, D., Ed.; Academic: New York, 1978; Vol. III, pp 1-165.

(39) (a) Kobayashi, H.; Hara, T.; Kaizu, Y. *Bull. Chem. Soc. Jpn.* **1972**, *45*, 2148-2155. (b) Kobayashi, H. *Adv. Biophys.* **1975**, *8*, 191-222. (c) Kobayashi, H.; Higuchi, T.; Eguchi, K. *Bull. Chem. Soc. Jpn.* **1976**, *49*, 457-463.

(40) Abragam, A.; Bleaney, B. In *Electron Paramagnetic Resonance of Transition Metal Ions*; Oxford University Press: London, 1970; p 399.

(41) Porterfield, W. W. In *Inorganic Chemistry*; Addison-Wesley: Reading, MA, 1984, p 439.